
**Separation Science and Technology**
Publication details, including instructions for authors and subscription information:
http://www.informaworld.com/smpp/title~content=t713708471

# Liquid Membranes: Advancing Reaction Zone Model for Finite Reactions

B. Janakiraman[a]
[a] DEPARTMENT OF CHEMICAL TECHNOLOGY, UNIVERSITY OF BOMBAY, BOMBAY, INDIA

**To cite this Article** Janakiraman, B.(1985) 'Liquid Membranes: Advancing Reaction Zone Model for Finite Reactions', Separation Science and Technology, 20: 5, 423 — 443
**To link to this Article: DOI:** 10.1080/01496398508060691
**URL:** http://dx.doi.org/10.1080/01496398508060691

SEPARATION SCIENCE AND TECHNOLOGY, **20**(5 & 6), pp. 423-443, 1985

# Liquid Membranes: Advancing Reaction Zone Model for Finite Reactions

B. JANAKIRAMAN

DEPARTMENT OF CHEMICAL TECHNOLOGY
UNIVERSITY OF BOMBAY
MATUNGA, BOMBAY 400019, INDIA



**Abstract**

An advancing reaction zone model has been proposed for a multiple emulsion liquid membrane for the case of simple permeation with finite reaction at the inner interphase. The model has been numerically solved and the effect of different system parameters on the rate of extraction and on the concentration profiles in the emulsion globule has been discussed.

## INTRODUCTION

Liquid membrane technology refers to a simultaneous extraction/stripping process which allows separation of mixtures to be achieved by means of a selective liquid membrane which allows only certain materials to permeate through it. Liquid membrane technology has been successfully employed in various fields including treatment of wastewater, separation of liquid or gas mixtures, gas-liquid reactions, as well as in the field of medicine. A considerable amount of experimental work has been done on liquid membranes (*1-7*) ever since they were first formulated by Li in the late 1960s. Over the past few years, several papers dealing with their theoretical aspects have appeared (*8-17*).

The advancing reaction front model proposed by Marr and co-workers (*9-11*) and by Li and co-workers (*12*) for multiple emulsion liquid membranes are valid only when the reaction occurring at the inner interphase of a multiple emulsion globule (interphase 1/2 in Fig. 1) is instantaneous. The reaction is so fast that the two reactants cannot co-



 0149-6395/85/2005-0423$3.50/0

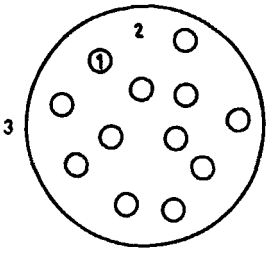


1 – ENCAPSULATED AQUEOUS PHASE

2 – OIL MEMBRANE PHASE

3 – CONTINUOUS EXTERNAL AQUEOUS PHASE

FIG. 1. Schematic diagram of an emulsion globule (w/o/w type).



exist. In this work an advancing reaction zone model is proposed for the case of finite reactions at the inner interphase and is solved by using some typical parameter values. This model has been worked out for the case of simple permeation with chemical reaction but can also be easily modified for carrier facilitated transport.

## MODELING MULTIPLE EMULSION LIQUID MEMBRANES

Figure 1 shows a schematic diagram for a w/o/w multiple emulsion globule. The following steps are involved in the case of simple permeation with reaction at the inner interphase (e.g., recovery of phenol from an aqueous phase by permeation through an oil membrane followed by an instantaneous reaction with NaOH at the inner 1/2 interphase. The phenolate ion formed is insoluble in the oil phase and hence remains trapped in the inner aqueous phase (Phase 1)):

(1) Diffusion from bulk Phase 3 to the 3/2 interphase
(2) Mass transfer across this interphase
(3) Transport through the membrane phase with simultaneous mass transfer into the inner Phase 1 droplets
(4) Reaction in the Phase 1 droplet

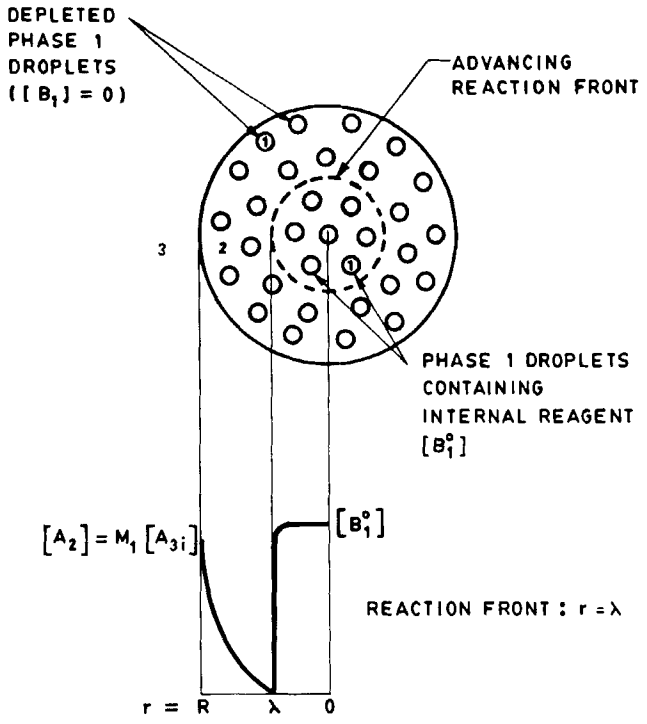


FIG. 2. Schematic representation of the advancing reaction front model.



This process was initially explained on the basis of the hollow sphere model which assumes that the inner Phase 1 droplets are in random motion within the globule (*1–5*). Kondo et al. (*8*) used this approach for $Cu^{2+}$ removal using benzyl acetone as a carrier. However, the membranes are generally made very viscous (3–100 cP) in order to have stable emulsions, and it is doubtful whether these droplets could move randomly (*11*). A more realistic approach is to consider them as fixed in the globule as in the advancing reaction front model for instantaneous reactions. This model was initially proposed by Marr and co-workers (*9–11*) for $Cu^{2+}$ removal with oxime carriers.

Li and co-workers (*12*) slightly modified this approach to set up equations for simple permeation with instantaneous reaction in spherical multiple emulsion membranes. The reaction of $A$ with the internal reagent $B$ in the Phase 1 droplets is assumed to be instantaneous and irreversible so that as soon as a Phase 1 droplet comes in contact with $A$, it is completely depleted of the internal reagent. This means that at any

time $t$ there is an outer zone where the Phase 1 droplets are depleted, and at the inner boundary of this zone there is a a reaction front ($r = \lambda$) where all $A$ is completely consumed by reaction. Thus the reaction front at $r$ equal to $\lambda$ separates an inner region ($0 < r < \lambda$) containing no $A$ from an outer region ($\lambda < r < R$) containing no internal reagent. In the outer region there is pure diffusion of $A$ as described by Fick's second law, followed by complete consumption by an instantaneous and irreversible reaction at $r$ equal to $\lambda$. As more and more of $B$ is consumed, $\lambda$ shifts into the interior toward $r = 0$. This is the basis of the advancing front model and is shown in Fig. 2.

Further assumptions made are that all the Phase 1 droplets have the same diameter, membrane leakage is neglible, and there is no mass transfer resistance for $A$ in Phase 3. These equations have been solved by using perturbation techniques, and the solutions have been successfully used to fit the experimental data for phenol removal from wastewaters.

More recently, Teramoto and co-workers have accounted for external mass transfer resistance (at the 3/2 interphase), membrane leakage, and internal droplet size distribution for removal of phenol, amines, and copper (*13–15*). In all the above cases the reaction at the inner interphase is instantaneous.



## ADVANCING REACTION ZONE MODEL

The advancing reaction front model, as already explained, holds only for instantaneous reactions at the 2/1 interphase. However, when this reaction is finite (low values of reaction rate constant; less than $10^2$ cm$^3$ Phase 1/g-mol · s), it is not possible to visualize an immediate depletion of B in phase 1 droplets. Hence it is necessary to consider the two steps of diffusion in the membrane and reaction in Phase 1 droplets as occurring in parallel, i.e., as $A$ diffuses in the liquid membrane, it is simultaneously taken up by the Phase 1 droplets. The latter step can be either mass transfer controlled or reaction limited. However, because finite kinetics are being considered and because mass transfer rates into Phase 1 droplets are very high due to the small droplet size ($k_{L1}a_1$ is about 140 for a droplet diameter of 2 μm), the uptake of $A$ into Phase 1 droplets can be taken as kinetically controlled. (Teramoto and co-workers (*14*) have taken this term to be mass transfer controlled in their model for instantaneous reactions, but because of high values of $k_La$, the concentration profiles will resemble that of the advancing front model.)

The approach for finite kinetics is therefore in contrast to that of the advancing front model for instantaneous reactions where the two steps are considered to occur in series. External mass transfer resistances at the 3/2 interphase are also accounted for here.

The following equations may be written for simple permeation with finite reaction at the inner 1/2 interphase.

*In Phase 3:*

$$-V_3 \frac{d[A_3]}{dt} = V_3 k_{L2} a_2 ([A_3] - [A_{3i}]) \tag{1}$$

$$= \frac{3}{R}(V_1 + V_2) D_0 \left.\frac{\partial [A_2]}{\partial r}\right|_{r=R} \tag{2}$$

$$t = 0, \qquad [A_3] = [A_{3i}] = [A_3^0] \tag{3}$$

$$t \geqslant 0, \qquad r = R, \qquad [A_{3i}] = [A_2^*] = [A_{2i}]/M_1 \tag{4}$$

These equations are obtained by equating the decrease in the concentration of $A$ in Phase 3 ($[A_3]$) to its rate of mass transfer from bulk to the 3/2 interphase, and this in turn is equated to its uptake by the emulsion globule. At time $t = 0$, the concentration of $A$ in Phase 3 is uniform throughout and equal to $[A_3^0]$. At all time $t$ the concentration of $A$ in Phase 3 at the interphase, $[A_{3i}]$, is related to the interfacial concentration of $A$ in Phase 2, $[A_{2i}]$, through the distribution coefficient $M_1$:

$$[A_{3i}] = [A_{2i}]/M_1 \tag{5}$$

The interfacial area between Phases 3 and 2, expressed as the surface area offered by Phase 2 drops per unit volume of Phase 3, $a_2$ is given by

$$a_2 = \frac{3l_2}{R} \tag{6}$$

where $R$ = radius of emulsion drop and

$$l_2 = \frac{V_1 + V_2}{V_3} \tag{7}$$

*In the Emulsion*: The diffusion of $A$ through the membrane may be described as

$$\frac{D_0}{r^2}\frac{\partial}{\partial r}\left[r^2\frac{\partial[A_2]}{\partial r}\right] = \frac{\partial[A_2]}{\partial t} + \frac{V_1}{V_1+V_2}k_{2w}[B_1][A_1] \tag{8}$$

or

$$D_0\frac{\partial^2[A_2]}{\partial r^2} + \frac{2}{r}D_0\frac{\partial[A_2]}{\partial r} = \frac{\partial[A_2]}{\partial t} + l_1k_{2w}[B_1]\frac{[A_2]}{M_2} \tag{9}$$

The depletion of $B$ in Phase 1 due to reaction with $A$ in Phase 1 may be expressed as

$$\frac{-\partial[B_1]}{\partial t} = k_{2w}[B_1][A_1] \tag{10}$$

$$= k_{2w}[B_1]\frac{[A_2]}{M_2} \tag{11}$$

Initial and boundary conditions are:

$$\text{For } t = 0: [B_1] = [B_1^0] \tag{12}$$

$$[A_2] = 0 \qquad \text{for } 0 \leqslant r \leqslant R \tag{13}$$

$$\text{For } t > 0: r = R,\ [A_{2i}] = [A_{3i}]M_1 \tag{14}$$

$$r = 0,\ \partial[A_2]/\partial r = 0 \tag{15}$$

Equation (9) has been obtained by a mass balance of $A$ in the emulsion and includes the consumption term for $A$ due to reaction with $B$ in Phase 1 droplets. As explained before, there is no mass transfer resistance for transfer of $A$ from Phase 2 to Phase 1 under the conditions of finite kinetics. Also, since the droplet sizes are very small (1–10 μm), there will be no concentration gradients of $A$ or $B$ within Phase 1. The concentrations of $A$ in Phases 2 and 1 are related through the distribution coefficient $M_2$. (Note: The concentration of $A$ in the membrane phase $[A_2]$ is defined per unit volume of the emulsion drop $(V_1 + V_2)$).

Since the internal reagent $B$ is trapped within Phase 1 droplets (which may be considered to be fixed in the emulsion globule), there is no diffusion term for $B$ in Eq. (10). The depletion of $B$ in Phase 1 is equated to its consumption by reaction with $A$ in this phase. (It may be stressed

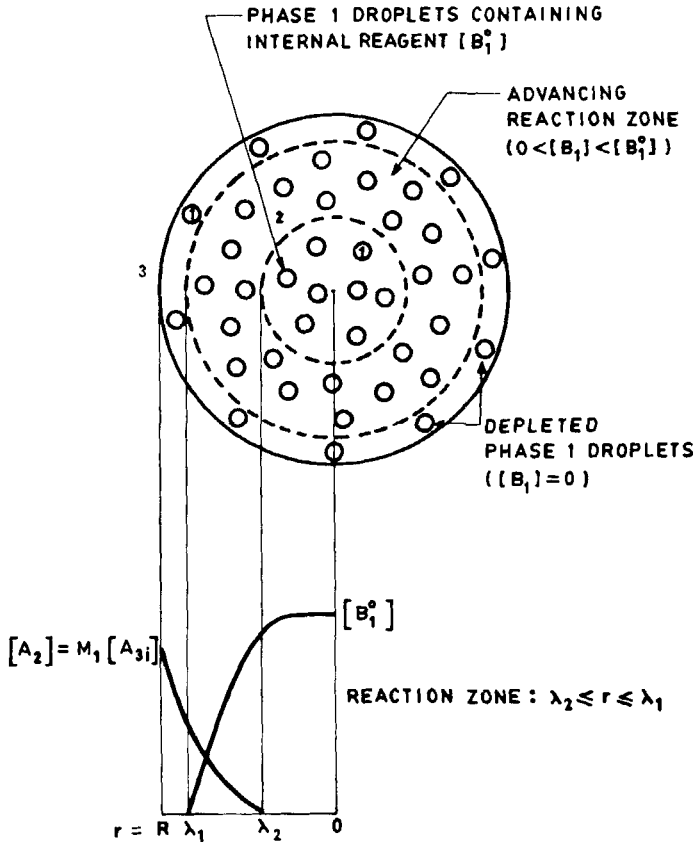


FIG. 3. Schematic representation of the advancing reaction zone model.

that writing $[B_1]$ as a continuous function of distance $r$ is an approximation because $B$ is actually compartmentalized within Phase 1 droplets and is not present in the membrane. However, since hold-up of Phase 1 is generally high (30% (v/v) or so) and the size of these droplets is very small (1–10) μm), the number of droplets is very large and they are close to each other. The discreet valued function $[B_1](r)$ is therefore approximated to a continuous function.)

At time $t = 0$, all the Phase 1 droplets have a concentration of $B$ equal to $[B_1^0]$. There is no $A$ present in Phases 2 and 1.

Equations (1)–(15) describe the process completely. As extraction proceeds, depletion of $B$ occurs initially in the outer region and gradually spreads inward. Over the region where $[B_1] = 0$, Eq. (9) reduces to Fick's

second law for transport of $A$. Further, the distance at which $[A_2]$ falls to zero depends on the relative rates of diffusion of $A$ in the membrane and the rate at which it is taken up by the phase 1 droplets. If $[A_2]$ becomes zero at a point before $r = 0$, then in that region where $[A_2]$ is equal to zero it is seen from Eq. (11) that there is no depletion of $B$. Thus, whereas in the instantaneous reaction regime there are only two regions separated by a sharp boundary (reaction front) which moves inward with time, here three zones may be visualized—an outer, completely depleted zone ($[B_1] = 0$); a central, partially depleted zone ($0 < [B_1] < [B_1^0]$); and an inner zone which does not show any depletion of $B$ ($[B_1] = [B_1^0]$, $[A_2] = 0$). The central partially depleted zone is where both $A$ and $B$ coexist, and the reaction takes place in this zone (which moves inward with time) in contrast to the sharp reaction boundary in the advancing reaction front model for instantaneous reactions. This model for finite reactions is therefore called the advancing reaction zone model. A schematic diagram of this model is shown in Fig. 3.



## NUMERICAL SOLUTION FOR THE ADVANCING REACTION ZONE MODEL

The above set of equations has been solved by the finite difference technique. The first step involves converting these equations to the dimensionless form.

Dimensionless concentration terms:

$$A3 = [A_3]/[A_3^0] \tag{16}$$

$$A3_i = [A_{3i}]/[A_3^0] \tag{17}$$

$$A2 = [A_2]/M_1[A_3^0] \tag{18}$$

$$B1 = [B_1]/[B_1^0] \tag{19}$$

Dimensionless distance:

$$X = r/R \tag{20}$$

Dimensionless time:

$$T = tD_0/R^2 \tag{21}$$

Dimensionless volume fractions:

$$l_2 = \frac{V_1 + V_2}{V_3} \tag{22}$$

$$l_1 = \frac{V_1}{V_1 + V_2} \tag{23}$$

Substitution of these dimensionless variables in Eqs. (1)–(15) gives the model in a dimensionless form.

*In Phase 3*:

$$-dA3/dT = H_1(A3 - A3_i) \tag{24}$$

$$(A3 - A3_i) = H_2 \left.\frac{\partial A2}{\partial X}\right|_{x=1} \tag{25}$$

$$T = 0, \qquad A3 = A3_i = 1 \tag{26}$$

$$T \geqslant 0, \qquad A3_i = A2_i \tag{27}$$

*In the Emulsion*:

$$\frac{\partial^2 A2}{\partial X^2} + \frac{2}{X}\frac{\partial A2}{\partial X} = \frac{\partial A2}{\partial T} + H_3(B1)(A2) \tag{28}$$

$$\frac{-\partial B1}{\partial T} = H_4(B1)(A2) \tag{29}$$

$$\text{For } T = 0, \qquad B1 = 1 \tag{30}$$

$$A2 = 0 \qquad \text{for } 0 \leqslant X \leqslant 1 \tag{31}$$

$$\text{For } T > 0, \qquad X = 1, \qquad A2_i = A3_i \tag{32}$$

$$X = 0, \qquad \partial A2/\partial X = 0 \tag{33}$$

The system parameters in these equations are given by

$$H_1 = \frac{3Rl_2k_{L2}}{D_0} \tag{34}$$

$$H_2 = \frac{D_0M_1}{Rk_{L2}} \tag{35}$$

$$H_3 = \frac{R^2l_1k_{2w}[B_1^0]}{D_0M_2} \tag{36}$$

TABLE 1
Parameter Values Used in the Model
($D_0 = 1.28 \times 10^{-6}$ cm$^2$/s, $d_1 = 2$ μm, $R_2 = 0.05$ cm, $[A_3^0] = 8.2 \times 10^{-3} M$)

| Run | $l_1$ | $l_2$ | $M_1 = M_2$ | $k_{L2} \times 10^3$ cm/s | $[B_1^0]$ $\left(\frac{\text{g} \cdot \text{mol}}{\text{cm}^3} \times 10^3\right)$ | $k_{2w}$ $\left(\frac{\text{cm}^3}{\text{g} \cdot \text{mol} \cdot \text{s}}\right)$ | $l_1 k_{2w} [B_1^0]$ ($s^{-1}$) | $k_{L1} a_1$ ($s^{-1}$) | Time for 70% extraction (min) |
|---|---|---|---|---|---|---|---|---|---|
| 2 | 0.363 | 0.067 | 0.7 | 1 | 0.5 | 1 | 0.181 | 140 | 58 |
| 3 | 0.363 | 0.067 | 0.7 | 1 | 0.5 | 10 | 1.81 | 140 | 52.7 |
| 4 | 0.363 | 0.067 | 0.7 | 1 | 0.5 | 100 | 18.1 | 140 | 48.9 |
| 5 | 0.363 | 0.067 | 0.7 | 1 | 2 | 0.1 | 0.0724 | 140 | 32.8 |
| 6 | 0.363 | 0.067 | 0.7 | 1 | 2 | 1 | 0.724 | 140 | 16.7 |
| 7 | 0.363 | 0.067 | 0.7 | 1 | 1 | 1 | 0.362 | 140 | 25.8 |
| 9 | 0.363 | 0.3 | 0.7 | 1 | 0.11 | 1 | 0.04 | 140 | 17.6 |
| 10 | 0.363 | 0.067 | 0.7 | 3 | 0.5 | 10 | 1.81 | 140 | 49.2 |
| 11 | 0.363 | 0.3 | 0.7 | 3 | 0.5 | 10 | 1.81 | 140 | 2.34 |
| 12 | 0.363 | 0.3 | 0.7 | 3 | 0.25 | 1 | 0.09 | 140 | 7.0 |
| 13 | 0.182 | 0.3 | 0.7 | 3 | 0.25 | 1 | 0.0453 | 70 | 13.8 |
| 14 | 0.363 | 0.067 | 1.4 | 1 | 0.5 | 1 | 0.181 | 140 | 34 |
| 15 | 0.363 | 0.067 | 5 | 1 | 0.5 | 1 | 0.181 | 140 | 17.3 |
| 16 | 0.363 | 0.067 | 0.35 | 3 | 0.5 | 10 | 1.81 | 140 | 97.5 |
| 17 | 0.363 | 0.067 | 1.4 | 3 | 0.5 | 10 | 1.81 | 140 | 25.2 |
| 18 | 0.363 | 0.067 | 0.7 | 5 | 0.5 | 10 | 1.81 | 140 | 48.3 |

$$H_4 = \frac{R^2 k_{2w} M_1 [A_3^0]}{D_0 M_2} \tag{37}$$

The solution of these equations should yield $A3$ as a function of time ($T$) and $A2$ and $B1$ as functions of time ($T$) and radial distance ($X$).

These partial differential equations have been solved by the method of finite differences (implicit method) (*18*).

## RESULTS

Table 1 gives the values of the parameters used for obtaining the output. These values of the parameters have been taken from the work of Li and co-workers (*12*), Marr and co-workers (*9–11*), and Teramoto and co-workers (*13–15*). For each set of input values the concentration profiles were obtained at different time levels.

Teramoto and co-workers (*13–15*) have measured the Phase 1 droplet size distribution using photographic and microscopic methods, and the average droplet size was observed to be between 1 to 5 μm. Now,

$$k_{L1} a_1 = \left(\frac{2D_0}{d_1}\right)\left(\frac{6l_1}{d_1}\right) \tag{38}$$

It is seen from Table 1 that $l_1 k_{2w} [B_1^0] \ll k_{L1} a_1$ for all the cases considered here, and hence the condition for finite reaction kinetics is satisfied.

Figure 4 gives the results of Run 2. It is seen from Fig. 4(a) that the mass transfer resistance for $A$ in Phase 3 (indicated by the difference in the values of $A3$ and $A3_i$) is significant in the beginning but becomes negligible toward the end when the rate of consumption of $A$ within the globule becomes low. The reaction zone initially extends over the region $0.7R \leqslant r \leqslant R$ and slowly advances inward. At around 70% level of extraction of $A$ from Phase 3, it covers the region $0.6R \leqslant r \leqslant 0.9R$ (Fig. 4b). The time for 75% extraction is 78.8 min ($T = 2.422$).

Examination of the results of all the runs showed that, depending on the parameter values, the reaction zone can extend over distances from less than 10% (approaching the instantaneous reaction profiles) to up to 100% of the emulsion globule radius. The effect of some of the parameters on the concentration profiles and the rate of extraction has been discussed below.

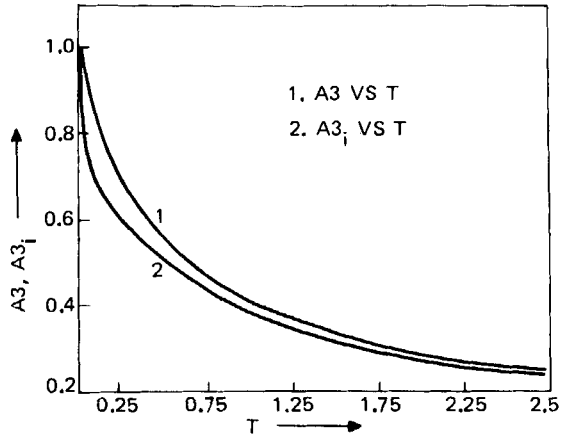


(a) DECREASE IN THE CONCENTRATION OF A IN THE BULK PHASE 3 AND AT THE INTERPHASE 3/2 WITH TIME

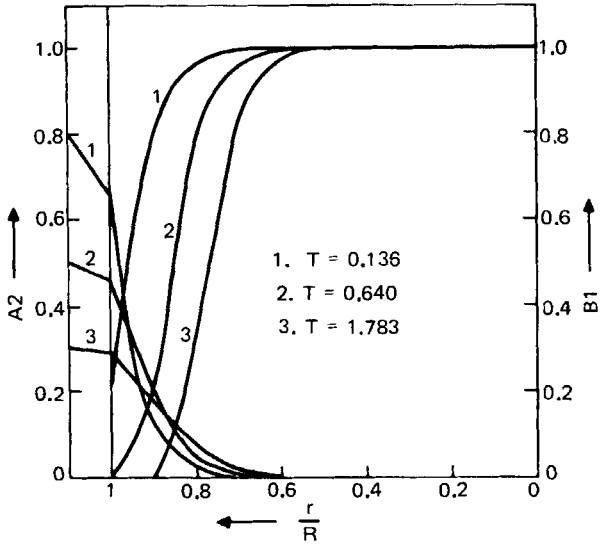


(b) CONCENTRATION PROFILES OF A AND B WITHIN THE EMULSION GLOBULE AT DIFFERENT TIMES

FIG. 4. Results of Run 2.

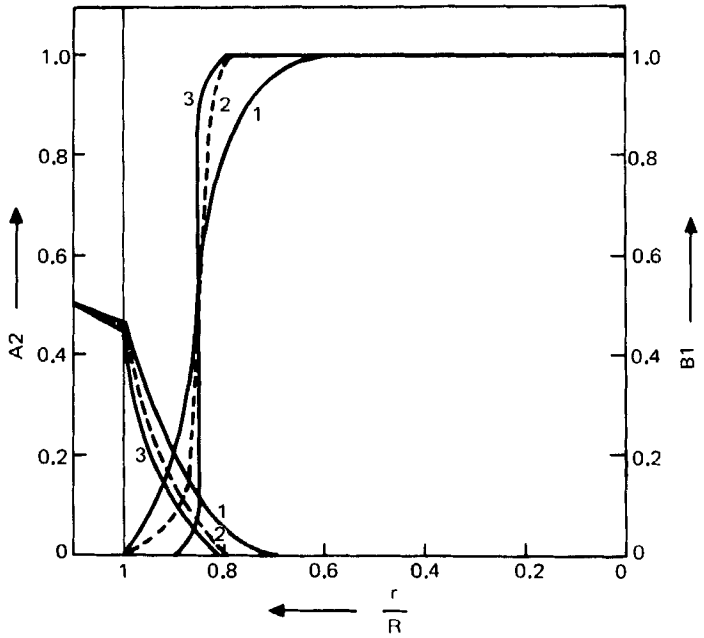


FIG. 5. Effect of rate constant. Concentration profiles at an extraction level of 50%. (1) For Run 2: $k_{2w}$ = 1 cm$^3$/g-mol · s ($T$ = 0.64 for $A3$ = 0.5). (2) For Run 3:P $k_{2w}$ = 10 cm$^3$/g-mol · s ($T$ = 0.532 for $A3$ = 0.5). (3) For Run 4: $k_{2w}$ = 100 cm$^3$/g-mol · s ($T$ = 0.496 for $A3$ = 0.5).



## 1. Effect of Rate Constant, $k_{2w}$

Figure 5 gives the concentration profiles of Runs 2, 3, and 4 when the extraction of $A$ from Phase 3 is 50% (the corresponding time levels are $T$ = 0.64, 0.532, and 0.496, respectively). These runs are for rate constant values of 1, 10, and 100 cm$^3$/g · mol · s with an initial internal reagent concentration, $[B_1^0]$, equal to 0.5 $M$ and all other parameters kept the same. As seen from Fig. 5, an increase in the rate constant narrows the zone of reaction and increases the extraction rate. For $k_{2w}$ = 1 cm$^3$/g · mol · s, the reaction zone extends over the region $0.7R \leqslant r \leqslant R$ until 50% extraction, after which the region around $r = R$ becomes limited in $[B_1^0]$ and the reaction zone advances inward to extend over $0.6R \leqslant r \leqslant 0.9R$ (see also Fig. 4). When the rate constant is increased by a factor of 10 (Run 3), the reaction zone becomes narrower. This is even more obvious in Run 4 where the concentration profiles closely resemble that of an instantaneous reaction. The reaction zone is narrowed down to a region around $r = 0.9R$, which then shifts inward to $r = 0.8R$ after 70% extraction.

The times for 75% extraction of $A$ from Phase 3 for $k_{2w}$ = 1, 10, and 100 $cm^3/g \cdot mol \cdot s$ are 78.8 min ($T$ = 2.422), 72 min ($T$ = 2.215), and 66.2 min ($T$ = 2.035), respectively.

Similar trends were observed on comparison of Runs 5 ($k_{2w}$ = 0.1 $cm^3/g \cdot mol \cdot s$) and 6 ($k_{2w}$ = 1 $cm^3/g \cdot mol \cdot s$) where the concentration of the internal phase reagent $[B_1^0]$, is 2 $M$. The time for 70% extraction of $A$ was observed to decrease from 32.8 to 16.7 min for an increase in the rate constant by a factor of 10.

## 2. Effect of Internal Phase Reagent Concentration, $[B_1^0]$

For $[A_3^0] = 8.2 \times 10^{-3}$ $M$, $l_1 = 0.067$, and $l_2 = 0.363$, the stoichiometric concentration of $[B_1^0]$ ($= [A_3^0]/l_1 l_2$) was calculated to be 0.337 $M$. However, the rate of extraction was found to be extremely slow when a stoichiometric amount of $B$ was used.

In Runs 2, 7, and 6 the rate constant was kept the same ($k_{2w}$ = 1 $cm^3/g \cdot mol \cdot s$) and the concentration of the internal phase reagent, $[B_1^0]$, was varied (Table 1).

Run 2: $[B_1^0]$ = 0.5 $M$ (1.48 times stoichiometric amount)
Run 7: $[B_1^0]$ = 1 $M$ (2.96 times stoichiometric amount)
Run 6: $[B_1^0]$ = 2 $M$ (5.93 times stoichiometric amount)

It was observed that the reaction zone narrows with increasing concentration of B in Phase 1. This result is readily explained by the fact that at low concentrations of $B$, the reaction rate in Phase 1 is also very low and hence $A$ penetrates deeper into the emulsion globule before it is fully consumed. On the other hand, a high value of $[B_1^0]$ causes $A$ to be completely consumed by reaction before it has time to diffuse inside, and for $[B_1^0]$ = 2 $M$ (Run 6) the reaction zone remains confined in the region $0.9R \leqslant r \leqslant R$. The rate of extraction increases with increasing $[B_1^0]$ as seen by the decreasing time values for 70% extraction: 58 min ($T$ = 1.783), 25.8 min ($T$ = 0.793), and 16.7 min ($T$ = 0.514) for $[B_1^0$ = 0.5, 1, and 2 $M$, respectively.

Table 2 summarizes the time for 75% extraction (i.e., for the concentration of $A$ in Phase 3 to fall to 0.25 of its initial value) for different combinations of rate constant and internal phase reagent concentration, $[B_1^0]$.

TABLE 2
Time for 75% Extraction of $A$ from Phase 3 for Different Values of $k_{2w}$ and $[B_1^0]$

| $\left(\frac{k_{2w}}{\frac{cm^3}{g \cdot mol \cdot s}}\right)$ | $\left(\frac{[B_1^0]}{\frac{g \cdot mol}{cm^3} \times 10^3}\right)$ | Time (min) |
|---|---|---|
| 1 | 0.5 | 78.8 |
| 10 | 0.5 | 75 |
| 100 | 0.5 | 66.2 |
| 1 | 1 | 31.6 |
| 10 | 1 | 28.4 |
| 100 | 1 | 27.2 |
| 0.1 | 2 | 38.7 |
| 1 | 2 | 19.6 |
| 10 | 2 | 16.7 |



### 3. Effect of Hold-up of Emulsion Phase, $l_2$

It is difficult to compare the sets of results with changing values of $l_2$ because the stoichiometric concentration of $B$ in Phase 1 also changes ($[B_1^0]_{\text{stoichiometric}} = [A_3^0]/l_1 l_2$), and, as seen earlier, the rate of extraction and the concentration profiles within the globule depend on the value of $[B_1^0]$ and also on how much higher it is than the stoichiometric value. For this reason, two cases have been considered. In the first case the stoichiometric excess of $[B_1^0]$ was kept the same in both runs, and in the second case the value of $[B_1^0]$ used was kept the same in both runs.

In the former case the value of $l_2$ was changed from 0.067 to 0.3 and the $[B_1^0]$ values used were 0.5 and 0.11 $M$, respectively, which are 1.48 times the respective stoichiometric amounts, 0.337 and 0.075 $M$. The rate constant ($k_{2w} = 1$ cm$^3$/g $\cdot$ mol $\cdot$ s) and other factors were kept the same (Runs 2 and 9). Figure 6 shows the concentration profiles for the two cases when the percent extraction is 50. It is seen that for the run where the $l_2$ value is higher, the penetration of $A$ is deeper and the reaction zone extends over a wider region ($0.4R \leqslant r \leqslant R$). The reason for the greater penetration is obviously the lower value of $[B_1^0]$ (equal to 0.11 $M$, though it is 1.48 times the stoichiometric value), as a result of which the reaction rate in Phase 1 and consequently the uptake of $A$ from Phase 2 to Phase 1 is low. The rate of extraction is, however, higher for greater hold-ups of the emulsion

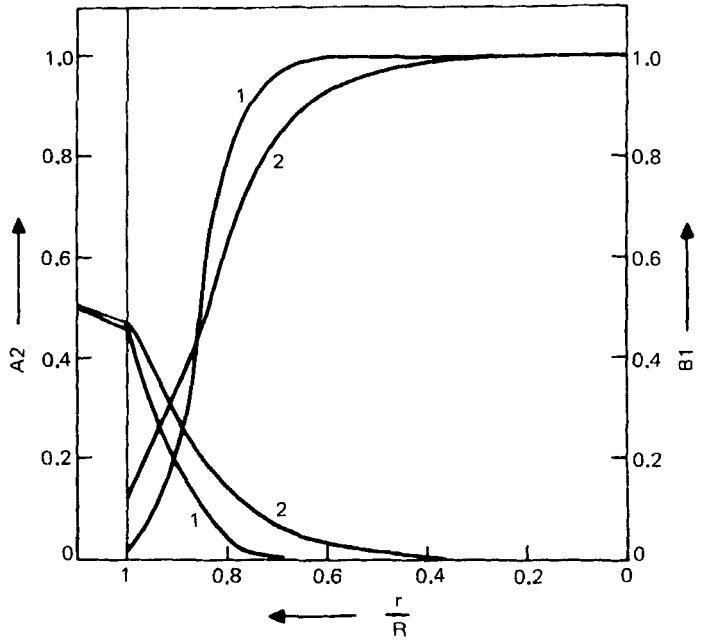


FIG. 6. Effect of hold-up of emulsion phase, $l_2$. Concentration profiles at an extraction level of 50%. (1) For Run 2: $l_2 = 0.067$ ($T = 0.64$ for $A3 = 0.5$). (2) For Run 9: $l_2 = 0.3$ ($T = 0.217$ for $A3 = 0.5$).



phase (higher $l_2$ values). The times for 75% extraction are 78.8 and 23.7 min for $l_2$ equal to 0.067 and 0.3, respectively.

In the second case the value of $l_2$ was again changed from 0.067 to 0.3, but the value of $[B_1^0]$ was kept the same for both cases (= 0.5 $M$) (Runs 10 and 11). This implies a stoichiometric excess of 1.48 for the case of $l_2$ equal to 0.067 (Run 10) and a stoichiometric excess of 6.67 for the case of $l_2$ equal to 0.3 (Run 11).

It was observed that the time for 70% extraction of $A$ from Phase 3 is 73.4 min for $l_2$ equal to 0.067, but is considerably reduced to 2.34 min when $l_2$ is increased to 0.3. The reaction zone was also found to be very much narrowed in the latter case and did not advance beyond $r = 0.9R$. The high stoichiometric excess of $[B_1^0]$ ensures complete consumption of $A$ in this narrow zone.

### 4. Effect of Hold-up of Phase 1, $l_1$

Here, too, difficulties arise in comparing results with different values of $l_1$ because the stoichiometric value of $[B_1^0]$ also varies. Runs 12 and 13 are

for $l_1$ values of 0.363 and 0.182, respectively, with $k_{2w}$ (= 1 cm$^3$/g · mol · s), $[B_1^0]$ (= 0.25 $M$), and other parameters having the same values in both runs. In the former case $[B_1^0]$ is 3.32 times the stoichiometric value, whereas in the latter case the $[B_1^0]$ value is only 1.66 times greater than the stoichiometric value. It was observed that for the case of a lower value of $l_1$ (= 0.182), the reaction zone extends over $0.2R \leqslant r \leqslant R$ whereas for the run with a higher value of $l_1$ (= 0.363) this zone is much narrower and extends only over $0.6R \leqslant r \leqslant R$ after 90% extraction of $A$ from Phase 3. A lower value of $l_1$ means lesser uptake of $A$ from Phase 2 into Phase 1 in the outer regions of the emulsion globule, thus resulting in a deeper penetration of $A$ into the globule. A lower stoichiometric excess of $[B_1^0]$ also contributes to a deeper penetration of $A$ into the globule. The time for 90% extraction of $A$ from Phase 3 increases from 16.1 min for $l_1$ equal to 0.363 to 48.9 min for $l_1$ equal to 0.182.



## 5. Effect of Distribution Coefficient of *A* between the Aqueous and Membrane Phases, $M_1$, $M_2$

The distribution coefficient of $A$ between the membrane phase and the aqueous phase at the 2/1 interphase ($M_2$) is generally slightly higher than the distribution coefficient at the 3/2 interphase ($M_1$) because of the presence of Reagent B in Phase 1. However, in all the runs considered in this work it has been assumed that $M_1$ and $M_2$ are equal.

In Runs 2, 14, and 15 the values of $M_1$ (and $M_2$) increase from 0.7 to 1.4 to 5 while keeping $k_{2w}$ (= 1 cm$^3$/g · mol · s), $[B_1^0]$ (= 0.5 $M$), and the other parameters the same. An increase in $M_1$ ($M_2$) implies greater solubility of $A$ in the membrane phase and lowered solubility in the aqueous Phases 3 and 1. An increase in the distribution coefficient increases the transfer of $A$ from Phase 3 to Phase 2 across the 3/2 interphase. A high value of $M_2$ within the emulsion globule means reduced uptake of $A$ from the membrane phase to the Phase 1 droplets. Thus, increasing the distribution coefficient would result in higher extraction rates of $A$ from Phase 3 and deeper penetration of $A$ within the globule as was observed in the results of Runs 2, 14, and 15. The time for 70% extraction of $A$ from Phase 3 was found to decrease from 58 to 34 to 17.28 min for a corresponding increase in the distribution coefficient ($M_1, M_2$) from 0.7 to 1.4 to 5. It was also observed that at the 70% extraction level for a distribution coefficient value of 5, the reaction zone extends over the entire emulsion globule ($0 \leqslant r \leqslant R$) but covers a much narrower region ($0.6R \leqslant r \leqslant R$) when the distribution coefficient is 0.7 (Run 2).

TABLE 3
Effect of Mass Transfer Coefficient of $A$, $k_{L2}$

| | $k_{L2}$ (cm/s) | | | | | |
|---|---|---|---|---|---|---|
| | $1 \times 10^{-3}$ | | $3 \times 10^{-3}$ | | $5 \times 10^{-3}$ | |
| $A3$ | $A3_i$ | $T$ | $A3_i$ | $T$ | $A3_i$ | $T$ |
| 0.8 | 0.6 | 0.082 | 0.72 | 0.064 | 0.75 | 0.053 |
| 0.7 | 0.58 | 0.172 | 0.66 | 0.136 | 0.68 | 0.127 |
| 0.6 | 0.53 | 0.307 | 0.57 | 0.262 | 0.58 | 0.253 |
| 0.5 | 0.46 | 0.532 | 0.49 | 0.469 | 0.493 | 0.460 |
| 0.4 | 0.38 | 0.919 | 0.39 | 0.838 | 0.394 | 0.820 |
| 0.3 | 0.29 | 1.621 | 0.295 | 1.504 | 0.298 | 1.477 |



Similar trends were observed in Runs 16, 10, and 17 where $M_1$ (and $M_2$) increase from 0.35 to 0.7 to 1.4, respectively, with $k_{2w}$ (= 10 cm$^3$/g · mol · s), $[B_1^0]$ (= 0.5 $M$), and the other parameters the same. The corresponding extraction times for 60% extraction of $A$ from Phase 3 decrease from 53.6 to 27.2 to 14.4 min, respectively.

## 6. Effect of Mass Transfer Coefficient of $A$ for Transfer from Phase 3 to Phase 2, $k_{L2}$

It was observed from the results of all the runs that even for those runs where the consumption of $A$ within the globule is slow (because of low values of $k_{2w}$ and $[B_1^0]$), there is a difference in the concentration of $A$ in the bulk Phase 3 ($A3$) and at the 3/2 interphase ($A3_i$ or $A2$ ($r = R$)), indicating that external mass transfer resistance at the 3/2 interphase is important (see Fig. 4a for Run 2). This resistance becomes more important when the consumption of $A$ within the globule is higher due to higher $k_{2w}$ and/or $[B_1^0]$ values when the difference between $A3$ and $A3_i$ becomes larger. However, toward the later stages of extraction, where the rate of consumption in the globule decreases, the mass transfer resistance also becomes less important.

Runs 3, 10, and 18 are for $k_{L2}$ values of $1 \times 10^{-3}$, $3 \times 10^{-3}$, and $5 \times 10^{-3}$ cm/s, respectively, with $k_{2w}$ (= 10 cm$^3$/g · mol · s), $[B_1^0]$ (= 0.5 $M$), and the other parameters kept the same. It was observed that the concentration profiles within the globules are not very different for these three cases. Table 3 gives the $A3$, $A3_i$, and time values at different stages of extraction for these three runs. As is evident, the mass transfer resistance is not very

significant in the later stages of extraction. It is also seen that increasing the $k_{L2}$ value reduces the difference in the $A3$ and $A3_i$ values and improves the extraction rate.

## CONCLUSIONS

1. For finite reactions at the inner 1/2 interphase, the kinetic factors must be considered.
2. The reaction occurs over a wide zone rather than at a reaction plane when the reaction is finite at the 1/2 interphase.
3. The width of the zone depends on the system parameters.



## SYMBOLS

| | |
|---|---|
| $A$ | substance to be extracted from the outer aqueous phase (Phase 3) |
| $[A_1]$ | concentration of $A$ in Phase 1 (g-mol/cm$^3$ phase 1) |
| $[A_2]$, $[A_{2i}]$ | concentration of $A$ in Phase 2 and at the interphase 3/2, respectively (g-mol/cm$^3$ emulsion globule volume) |
| $[A_3]$, $[A_{3i}]$ | concentration of $A$ in Phase 3 and at the interphase 3/2, respectively (g-mol/cm$^3$ Phase 3) |
| $[A_3^0]$ | concentration of $A$ in Phase 3 at time $t = 0$ (g-mol/cm$^3$ Phase 3) |
| $[A_2^*]$ | $= [A_{2i}] = M_1[A_{3i}]$ (g-mol/cm$^3$ emulsion globule volume) |
| $a_1$ | interfacial area offered by Phase 1 droplets (cm$^2$/cm$^3$ emulsion globule volume) |
| $a_2$ | interfacial area offered by emulsion globule (cm$^2$/cm$^3$ Phase 3) |
| $A2$, $A3$, $A3_i$ | dimensionless concentration of $A$ in emulsion globule, in Phase 3, and at interphase 3/2, respectively |
| $B$ | internal phase reagent |
| $[B_1]$, $[B_1^0]$ | concentration of $B$ in Phase 1 at any time $t$ and time $t = 0$, respectively (g-mol/cm$^3$ Phase 1) |
| $B1$ | dimensionless concentration of $B$ in Phase 1 |
| $D_0$ | diffusivity of $A$ in Phase 2 (cm$^2$/s) |
| $d_1$ | diameter of Phase 1 droplet (cm) |
| $H_1$, $H_2$, $H_3$, $H_4$ | system parameters as defined by Eqs. (34) to (37) |
| $k_{L1}$ | mass transfer coefficient for transfer of $A$ from Phase 2 to 1 (cm/s) |

| | |
|---|---|
| $k_{L2}$ | mass transfer coefficient for transfer of $A$ from Phase 3 to 2 (cm/s) |
| $k_{2w}$ | second-order reaction rate constant ($cm^3$ Phase 1/g-mol · s) |
| $l_1$ | $= \dfrac{V_1}{V_1 + V_2}$ |
| $l_2$ | $= \dfrac{V_1 + V_2}{V_3}$ |
| $M_1$ | distribution coefficient for $A$ between Phases 3 and 2 |
| $M_2$ | distribution coefficient for $A$ between Phases 1 and 2 |
| $r$ | radial distance in emulsion globule (cm) |
| $R$ | radius of emulsion globule |
| $t$ | time (s) |
| $T$ | $= tD_0/R^2$ (dimensionless time) |
| $V_1, V_2, V_3$ | volumes of Phases 1, 2, and 3, respectively ($cm^3$) |
| $X$ | $= r/R$ (dimensionless distance) |

## Greek

| | |
|---|---|
| $\lambda$ | distance of reaction front from the center of the globule (cm) |
| $\lambda_1, \lambda_2$ | distances of outer and inner boundaries of advancing reaction zone from the center of the globule (cm) |



## REFERENCES


1. T. Kitagawa, Y. Nishikawa, J. W. Frankenfeld, and N. N. Li, *Environ. Sci. Technol., 11*, 602 (1977).
2. N. N. Li, *J. Membr. Sci., 3*, 265 (1978).
3. R. P. Cahn, N. N. Li, and R. M. Minday, *Environ. Sci. Technol., 12*, 1051 (1978).
4. R. P. Cahn, J. W. Frankenfeld, N. N. Li, D. Naden, and K. N. Subramanian, *Recent Developments in Separation Science*, Vol. 6, CRC Press, Florida, 1981.
5. J. W. Frankenfeld, R. P. Cahn, and N. N. Li, *Sep. Sci. Technol., 16*, 385 (1981).
6. S. S. Davies, *Chem. Ind.*, p. 683 (1981).
7. N. N. Li, *Chem. Eng., 370*, 325 (1981).
8. K. Kondo, K. Kita, I. Koida, J. Irie, and E. Nakashio, *J. Chem. Eng. Jpn., 12*, 203 (1979).
9. R. Marr, H. J. Bart, and A. Bouvier, *Ger. Chem. Eng., 4*, 209 (1981).
10. R. Marr, H. J. Bart, and M. Siehenhofer, *Proc. Int. Solv. Extr. Conf.*, Vol. 2, Sec. 12, 1980.

*11.* R. Marr and A. Kopp., *Int. Chem. Eng., 22*, 44 (1982).
*12.* W. S. Ho, T. A. Hatton, E. N. Lightfoot, and N. N. Li, *AIChE J., 28*, 662 (1982).
*13.* M. Teramoto, H. Takihana, M. Shibutani, T. Yausa, Y. Miyake, and H. Teranishi, *J. Chem. Eng. Jpn., 14*, 122 (1981).
*14.* M. Teramoto, H. Takihana, M. Shibutani, T. Yuasa, and N. Hara, *Sep. Sci. Technol., 18*, 397 (1983).
*15.* M. Teramoto, T. Sakai, K. Yanagawa, M. Ohsuga, and Y. Miyake, *Ibid., 18*, 735 (1983).
*16.* M. Teramoto and H. Tanimoto, *Ibid., 18*, 871 (1983).
*17.* M. Teramoto, T. Sakai, K. Yanagawa, and Y. Miyake, *Ibid., 18*, 985 (1983).
*18.* B. Carnahan, H. A. Luther, and J. O. Wilkes, *Applied Numerical Methods*, Wiley, New York, 1969, p. 429.

*Received by editor December 12, 1984*